Pré-Publicações do Departamento de Matemática
Universidade de Coimbra
Preprint Number 28–22

DRUG DELIVERY TO THE ANTERIOR SEGMENT OF THE EYE ENHANCED BY ULTRASOUND - MODELING AND SIMULATION

E. AZHDARI, E. EMAMI AND J. A. FERREIRA

Abstract: Transcorneal drug delivery has been used to treat eye diseases of both segments of the eye: anterior and posterior segments. Due to the low corneal permeability, this drug administration route has been shown to be very ineffective. Ultrasound has been used to increase the corneal drug transport.

In this paper we consider a system of partial differential equations (PDEs) defined by a wave equation to describe the propagation of the pressure wave generated by a transducer, a convection-diffusion-reaction equation for the drug transport in each layer of the cornea - epithelium, stroma and endothelium. The last equations are linked with the acoustic pressure through the diffusion coefficient and the convective velocity. The system of PDEs is completed with convenient interface conditions, initial and boundary conditions. The initial boundary value problem is studied from analytical point of view and the qualitative behaviour is numerically illustrated. The results confirm the effectiveness of ultrasound as enhancer of the drug delivery through the cornea.

AMS Subject Classification (2000): 65M20, 65M60.

1. Introduction

Traditionally, topical drops are the most popular drug delivery procedure to the eye. Drug delivery to the eye is a very difficult task due to the eye defenses that protect it from the exterior environment. The reflex blinking and the tear fluid turnover contribute to the loss of 60% of the applied active agents and, consequently, for the inefficiency of the eye drops as a drug delivery system ([9]).

The first barrier that drug must face is the cornea due to its low permeability. The cornea is composed by three different layers: the epithelium, the stroma and the endothelium. These layers present different properties. The two first layers, epithelium and stroma, contain intracellular compartments and extracellular micro-domains being the first one composed by cells and the second one by extracellular matrix (ECM). Collagen is the main

Received October 5, 2022.

This work was partially supported by the Centre for Mathematics of the University of Coimbra-UIDB/00324/2020, funded by the Portuguese Government through FCT/MCTES.

ingredient in the ECM composition which is homogeneously distributed and is responsible by the transparency and by the organized structure of the stroma. The endothelium is a single layer of cells ([4]). Due to the lipophilic nature of the epithelium, the first layer is a barrier to the hydrophilic drugs while the stroma, due to its hydrophilic nature, is a barrier to the lipophilic drugs. These features are responsible by the low permeability of the cornea to lipophilic and hydrophilic drugs.

To increase corneal permeability and, consequently, to enhance the drug transport, ultrasound has been used. Without being exhaustive we mention [6], [8], [14], [15], [19], [22] and [23]. The ultrasonic transducer generates pressure waves that, as they propagate, they change the behaviour of the microbubbles present in the target tissue. Acoustic pressure waves with frequency higher than the audible limit (approximately 20 kHz) induce the so called cavitation phenomenon- expansion and contraction of the microbubbles. This phenomenon can be stable if the bubbles do not collapse. In this case, as a result of the shear stress and the microstreaming around bubbles oscillating, the rupture of the cell membranes can occur. If the bubbles collapse, the cavitation is said inertial, and, in this case, high speed liquid jets that are able to create pits in the biological tissue appear (see for instance [8] and [23]).

The waves propagation lead to pressure gradient that, with the oscillatory movement of the microbubbles, induce a convective transport ([11]). It should be pointed out that, depending on the ultrasound intensity, an increasing on the temperature in the target tissue can be observed ([16], [24]).

In several experiments involving ultrasound, different histological modifications of the corneal layers were observed depending on the characteristics of the protocols used. For instance, in [15], [22] and [23], are included experiments where no structural alteration of the stroma and endothelium were observed. In ([1]) the deliver of macromolecules thought the cornea is studied and no structural alterations were observed. However, if the ultrasound protocols lead to significant changes on the temperature, as in high intensity focused ultrasound, then temporal structural collagen changes take place (see for instance [20]).

In this paper we consider a reservoir containing a solution, a solvent and drug, in contact with the epithelium as represented in Figure 1.

In Figure 2 we present a representation of the cornea that will be considered later. In this figure, the main three corneal layers : epithelium (Ω_{ep}),

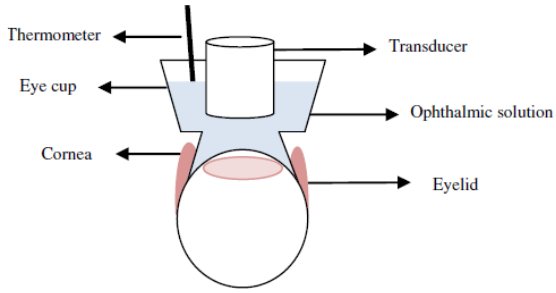

FIGURE 1. A schematic representation of the physical model (see [15]).

stroma (Ω_s) and endothelium (Ω_e) are highlighted. The boundaries and the interfaces between the corneal layers are also included. By Ω we represent the corneal region. The boundary of Ω in contact with the anterior chamber is denoted by Γ_e. By $\Gamma_{i,j}$ we represent the interface between the layers Ω_i and Ω_j. By $\Gamma_{i,j}$ we denote the left ($j = \ell$) and right ($j = r$) boundaries of Ω_i.

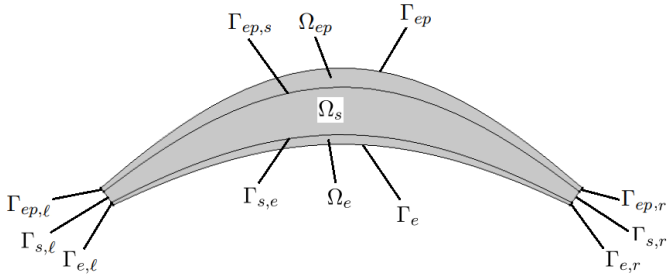

FIGURE 2. A schematic representation of the spatial domain Ω.

The acoustic pressure waves generated by the transducer (see Figure 1) propagate through the solution, reach the cornea with a known intensity, and then propagate through the corneal layers. We consider that the ultrasound protocol does not lead to a significant increasing on the temperature.

We assume that the intensity of the pressure waves through the corneal layers is described by the wave equation and, to maintain a general presentation, the waves propagation speed is different in the three corneal layers, that is

$$\frac{\partial^2 p_i}{\partial t^2} = \nu_i \Delta p_i \text{ in } \Omega_i \times (0, T], \tag{1}$$

for $i = ep, s, e$. In (1), T is a final time, $p_i(x,t)$ denotes the pressure wave intensity at $x \in \Omega_i$ at time t, and ν_i represents the pressure wave speed in Ω_i.

In what follows we use the following notation: if $u : \overline{\Omega} \times [0,T] \to \mathbb{R}$, then, for $t \in [0,T]$, by $u(t)$ and $u^{(j)}(t)$, $j = 1, 2$, we represent the following functions $u(t) : \overline{\Omega} \to \mathbb{R}$, $u(t)(x) = u(x,t)$, and $u^{(j)}(t) : \Omega \to \mathbb{R}$, $u^{(j)}(t)(x) = \dfrac{\partial^j u}{\partial t^j}(x,t)$.

Equation (1) is completed with the following conditions:

(1) Initial conditions:

$$p_i'(0) = p_i(0) = 0 \text{ in } \Omega_i, \tag{2}$$

for $i = ep, s, e$, that means that the ultrasound waves are generated at the initial time $t = 0$;

(2) Boundary conditions:

- the acoustic pressure is assumed to be known on the boundary Γ_{ep}

$$p_{ep}(t) = p_{\Gamma_{ep}}(t), \text{ on } \Gamma_{ep}, \tag{3}$$

- the other boundaries do not interfere with the acoustic waves propagation, that is,

$$\nabla p.\eta = 0 \text{ on } \Big(\bigcup_{j=ep,s,e,q=\ell,r} \Gamma_{j,q} \cup \Gamma_e \Big) \times (0,T], \tag{4}$$

where η denotes the unitary exterior normal to the boundaries $\Gamma_{j,q}$ and Γ_e;

(3) interface condition:

- continuity of p on $\Gamma_{\ell,q}, \ell = ep, s, q = s, e$,
-

$$\nu_{ep} \nabla p_{ep}.\eta_{ep} + \nu_s \nabla p_s.\eta_s = 0 \text{ on } \Gamma_{ep,s} \times (0,T], \tag{5}$$

and

$$\nu_s \nabla p_s.\eta_s + \nu_e \nabla p_e.\eta_e = 0 \text{ on } \Gamma_{s,e} \times (0,T]. \tag{6}$$

In (5), η_i is the exterior unitary normal to Ω_i on $\Gamma_{i,j}$.

The three corneal layers are histologically significantly different. Due to the cavitation phenomenon generated by the propagation of the acoustic pressure waves, temporary pores arise in the corneal layers. In [6], a mathematical law to describe the porosity changes that occur in the cornea when the acoustic pressure waves propagate within it is proposed . If ϕ_j denotes the porosity of

the layer Ω_j induced by the acoustic pressure intensity p_j defined by (1)-(6), then

$$\phi_j \;=\; \phi_{j_0} e^{\beta_{j_m}(p_j - p_0)}, \tag{7}$$

where ϕ_{j_0} represents the porosity at a reference pressure p_0 and β_{j_m} is a normalization constant.

If a drug dispersed in the solution (see Figure 1) enters in the epithelium, then its transport through the corneal layers is induced by the gradient of the acoustic pressure and by the gradient of the drug concentration. Then the drug transport occurs by diffusion and by the active transport due to the convective field generated by the pressure gradient (see for instance the general review [17]). In what concerns, the active transport, Darcy's law defines the convective velocity v_j in each layer

$$v_j = -\frac{k_j}{\mu}\nabla p_j, \tag{8}$$

where μ represents the viscosity, k_j represents the permeability of medium Ω_j, $j = ep, s, e,$. According to [10], the permeability, the porosity and the tortuosity of the τ_j are related by the following identity

$$k_j = \frac{\phi_j^3}{\mathcal{K}\tau_j^2 A_j^2}, \tag{9}$$

where A_j is the specific surface area and $\mathcal{K}$ is the Kozeny coefficient.

Let $c_j(x,t)$ denotes the drug concentration in $x \in \Omega_j$ at time t and let $J_j(x,t)$ be the drug flux

$$J_j = -D_j \nabla c_j + v_j c_j. \tag{10}$$

In what concerns the passive transport, the drug diffusion coefficient D_j in each layer Ω_j, satisfies

$$D_j \;=\; D_{j_0}\phi_j, \tag{11}$$

where D_{j_0} represents the molecular diffusion coefficients in the layer Ω_j, respectively (see for instance [6, 12]).

Then the dynamic of the drug molecules in the layer Ω_j is defined by

$$\frac{\partial c_j}{\partial t} + \nabla.(c_j v_j) = \nabla.(D_j \nabla c_j) - c_{\ell a} c_j \quad \text{in } \Omega_j \times (0,T], \tag{12}$$

for $j = ep, s, e$. In (12), $c_{\ell a}$ denotes the drug clearance rate in Ω that we assume constant.

The system of partial differential equations (12) is complemented with initial condition

$$c_j(0) = 0 \text{ in } \Omega_j,\ j = ep, s, e, \tag{13}$$

and boundary conditions

$$\begin{cases} c_{ep} = c_R \text{ on } \Gamma_{ep} \times (0,T], \\ J_{ep}.\eta = 0 \text{ on } (\cup_{q=\ell,r}\Gamma_{ep,q}) \times (0,T], \\ J_s.\eta = 0 \text{ on } (\cup_{q=\ell,r}\Gamma_{s,q}) \times (0,T], \\ J_e.\eta = 0 \text{ on } (\cup_{q=\ell,r}\Gamma_{e,q}) \times (0,T], \\ J_e.\eta = k_e c_e \text{ on } \Gamma_e \times (0,T]. \end{cases} \tag{14}$$

In (14), c_R is the drug concentration on Γ_{ep} given by the drug concentration in the solute in the reservoir in contact with the cornea. The last equation in (14) means that the drug that enters in the anterior chamber depends on the permeability k_e of Γ_e and of the drug that reaches this boundary. Finally, to complete our mathematical model we need to impose interface conditions

$$\begin{cases} J_{ep}.\eta_{ep} = k_{ep,s}(c_{ep} - c_s) \text{ on } \Gamma_{ep,s} \times (0,T], \\ J_{ep}.\eta_{ep} = -J_s.\eta_s \text{ on } \Gamma_{ep,s} \times (0,T], \\ J_s.\eta_s = k_{s,e}(c_s - c_e) \text{ on } \Gamma_{s,e} \times (0,T], \\ J_s.\eta_s = -J_e.\eta_e \text{ on } \Gamma_{s,e} \times (0,T]. \end{cases} \tag{15}$$

In (15), $k_{i,j}$ represents the mass transfer coefficient between the layers Ω_i and Ω_j. The discontinuities on the drug concentration on the interfaces regions are consequence of the different histological characteristics of the different layers that determine different ultrasound effects influencing the drug transport.

In what concerns the mathematical modeling of drug delivery enhanced by ultrasound, we observe that in [7] is studied a system of PDEs composed by a wave equation for the ultrasound intensity and a convection-diffusion equation for the drug concentration that can be used to model the drug transport in a target tissue stimulated by ultrasound. In [6], the authors study the drug transport through the cornea where ultrasound is used to increase the corneal porosity. Assuming known acoustic pressure waves intensities, a diffusion equation is used to describe the drug concencentration distribution in the corneal layers. In the context of drug delivery in solid tumors enhanced by high intensity focused ultrasound, in [21], a detailed mathematical description of the drug dynamics is presented. No detailed description of the acoustic wave propagation is included. Instead, the authors consider a set of explicit formulas to obtain an approximation for the acoustic pressure waves

intensities. In [18], the coupling of the drug dynamics in a porous medium with the acoustic wave propagation induced by high intensity ultrasound is studied. A third order in time modified Westervelt equation is used to describe the waves generated by the ultrasound device.

To the best of our knowledge, in the present paper is firstly introduced a set of PDEs that can be used to describe the drug transport through the cornea enhanced by ultrasound. In the set of equations, the change of the porosity induced by the propagation of the pressure waves is taken into account. Convection-diffusion-reaction equations for the drug concentration in the different corneal layers are considered. Here, the convective velocity is given by Darcy's law where the permeability depends on the acoustic pressure intensity. In the coupling between different layers, convenient interface conditions for the pressure and concentration are used. From theoretical point of view, our main interest is to generalize the Conservation Energy Principle, that holds for the wave equation, to the acoustic pressure waves intensity in the corneal layers. Energy bounds are also studied as well as their influence on the energy bounds for the drug concentration. From numerical point of view, piecewise linear finite element approximations for the acoustic pressure intensity and for the drug concentration will be studied. These finite element approximations preserve the qualitative properties the initial solutions: acoustic pressure intensity and drug concentration.

The paper is organized as follows. In Section 2, we establish the energy conservation for the acoustic pressure intensity and the stability of the IBVP (1)-(6). Taking into account the results of the previous section, in Section 3 we conclude the stability of the IBVP (7)-(15). Section 4 is devoted to the numerical simulation. The piecewise linear finite element approximations for the acoustic pressure and drug concentrations will be considered. Numerical experiments illustrating the behaviour of the acoustic pressure intensity and the drug concentration are also included. Finally, some conclusions are presented in Section 5.

2. Energy conservation and stability for the acoustic pressure

We establish in what follows the stability of the IBVP (1)-(6). Let $L^2(\Omega_j)$ be the usual space where we consider the usual L^2 inner product $(.,.)_{L^2(\Omega_j)}$ and the corresponding norm $\|.\|_{L^2(\Omega_j)}$, for $j = ep, s, e$.

Let $(p_{ep}, p_s, p_e) \in H^2(0,T, \prod_{i=ep,s,e} L^2(\Omega_i)) \cap L^2(0,T, \prod_{i=ep,s,e} H^1(\Omega_i))$ be such that $p_{ep} = p_{\Gamma_{ep}}$ on $\Gamma_{ep} \times (0,T]$ and

$$\sum_{i=ep,s,e} (p_i''(t), u_i)_{L^2(\Omega_i)} + \sum_{i=ep,s,e} \nu_i (\nabla p_i(t), \nabla u_i)_{[L^2(\Omega_i)]^2} = 0,\ t \in (0,T], \quad (16)$$

for all $(u_{ep}, u_s, u_e) \in H^1_{\Gamma_{ep},0}(\Omega_{ep}) \times H^1(\Omega_s) \times H^1(\Omega_e)$, and

$$p_i'(0) = p_i(0) = 0 \text{ in } L^2(\Omega_i), i = ep, s, e. \quad (17)$$

In (16), $H^1_{\Gamma_{ep},0}(\Omega_{ep}) = \{u \in H^1(\Omega_{ep}) : u = 0 \text{ on } \Gamma_{ep}\}$.

By $E_p(t)$ we denote total energy defined

$$E_p(t) = \sum_{i=ep,s,e} \Big(\|p_i'(t)\|^2_{L^2(\Omega_i)} + \nu_i \|\nabla p_i\|^2_{[L^2(\Omega_i)]^2} \Big), p \in [0,T], \quad (18)$$

where $\|p_i'(t)\|^2_{L^2(\Omega_i)}$ represents the kinetic energy and $\nu_i \|\nabla \omega_i\|^2_{[L^2(\Omega_i)]^2}$ the potential energy. In the next result we prove that if the corneal system is isolated, that is $p_{\Gamma_{ep}} = 0$, then the energy E_p is constant in time.

Proposition 1. *Let (p_{ep}, p_s, p_e) be solutions of the IBVP (16), (17), with $p_{\Gamma_{ep}} = 0$, belonging to $C^2([0,T], \prod_{i=ep,s,e} L^2(\Omega_i)) \cap C^1([0,T], \prod_{i=ep,s,e} H^1(\Omega_i))$. Then*

$$E_p(t) = E_p(0), t \in [0,T]. \quad (19)$$

Proof: Considering (16) for (p_{ep}, p_s, p_e) and taking $u_i = p_i'(t)$, $i = ep, s, e$, we obtain

$$\sum_{i=ep,s,e} \Big((p''(t), p_i'(t)(t))_{L^2(\Omega_i)} + \nu_i (\nabla p_i(t), \nabla p_i'((t))_{[L^2(\Omega_i)]^2} \Big) = 0,$$

that can be written in the following equivalent form

$$E_p'(t) = 0, t \in (0,T]. \quad (20)$$

The identity (20) easily leads to (19).

■

As a corollary we have the following stability results:

Corollary 1. *Let (p_{ep}, p_s, p_e) and $(\tilde{p}_{ep}, \tilde{p}_s, \tilde{p}_e)$ be solutions of the IBVP (16), (17) belonging to $C^2([0,T], \prod_{i=ep,s,e} L^2(\Omega_i)) \cap C^1([0,T], \prod_{i=ep,s,e} H^1(\Omega_i))$ where the initial conditions for $(\tilde{p}_{ep}, \tilde{p}_s, \tilde{p}_e)$ are defined by*

$$\tilde{p}_i'(0) = \psi_i, \tilde{p}_i(0) = \phi_i \text{ in } L^2(\Omega_i), \quad (21)$$

with $\psi_i \in L^2(\Omega_i), \phi_i \in H^1(\Omega_i), i = ep, s, e.$

Then for $\omega_i(t) = p_i(t) - \tilde{p}_i(t)$, $i = ep, s, e$, *holds the following*

$$\begin{aligned} &\sum_{i=ep,s,e} \Big(\|\omega_i'(t)\|^2_{L^2(\Omega)} + \nu_i \|\nabla \omega_i\|^2_{[L^2(\Omega_i)]^2} \Big) \\ &\qquad = \sum_{i=ep,s,e} \Big(\|\psi_i\|^2_{L^2(\Omega_i)} + \nu_i \|\nabla \phi_i\|^2_{[L^2(\Omega_i)]^2} \Big), t \in [0,T]. \end{aligned} \tag{22}$$

Moreover, there exists a positive constant C_T *such that*

$$\sum_{i=ep,s,e} \|\omega_i(t)\|^2_{H^1(\Omega)} \leq C_T \sum_{i=ep,s,e} \Big(\|\psi_i\|^2_{L^2(\Omega_i)} + \nu_i \|\nabla \phi_i\|^2_{[L^2(\Omega_i)]^2} \Big), t \in [0,T]. \tag{23}$$

Proof: The identity (22) follows directly from Proposition 1. To conclude (23) we remark that there exists a positive constant C such that

$$\|\omega_i(t)\|^2_{L^2(\Omega_i)} \leq C \Big(\int_0^t \|\omega_i'(s)\|^2_{L^2(\Omega_i)} ds + \|\omega_i(0)\|^2_{L^2(\Omega_i)} \Big), t \in [0,T], i = ep, s, e.$$

■

Corollary 2. *There exists at most one solution of the IBVP (16), (17) in* $C^2([0,T], \prod_{i=ep,s,e} L^2(\Omega_i)) \cap C^1([0,T], \prod_{i=ep,s,e} H^1(\Omega_i)) \cap C^0([0,T], \prod_{i=ep,s,e} H^2(\Omega_i))$.

Proof If (p_{ep}, p_s, p_e) and $(\tilde{p}_{ep}, \tilde{p}_s, \tilde{p}_e)$ are solutions of the IBVP (16), (17) satisfying the required smoothness assumption, then, for $\omega_i(t) = p_i(t) - \tilde{p}_i(t), i = ep, s, e$, we have

$$\omega_i'(t) = 0, \ \nabla \omega_i(t) = 0 \text{ a.e. in } \Omega_i, i = ep, s, e.$$

As $\omega_{ep}(t) = const$ a.e. in Ω_{ep}, $\omega_{ep}(t) = 0$ on Γ_{ep} and, taking into account that $H^2(\Omega_{ep})$ is embedded in $C(\overline{\Omega}_{ep})$, $\omega_{ep}(t) \in C(\overline{\Omega}_{ep})$, we obtain $\omega_{ep}(t) = 0$ in $\overline{\Omega}_{ep}$, for $t \in [0,T]$. Analogously, we conclude that $\omega_i(t) = 0$ in $\overline{\Omega}_i, i = s, e$, and $t \in [0,T]$.

■

The solution of the non homogeneous problem (16), (17) can be obtained solving a homogeneous one. In fact, let us suppose that we can extend $p_{\Gamma_{ep}}$ to $\Omega \times [0,T]$. Let p_{ex} be such extension. Let $w_i(t) = p_i(t) - p_{ex}(t), i = ep, s, e.$

We observe that $w_{ep}(t) \in H^1_{\Gamma_{ep},0}(\Omega)$ we have

$$\sum_{i=ep,s,e} \Big((w_i''(t), u_i)_{L^2(\Omega_i)} + \nu_i (\nabla w_i(t), \nabla u_i)_{[L^2(\Omega_i)]^2} \Big) = - \sum_{i=ep,s,e} (p_{ex}''(t), u_i)_{L^2(\Omega_i)} - \sum_{i=ep,s,e} \nu_i (\nabla p_{ex}(t), \nabla u_i)_{[L^2(\Omega_i)]^2},\ t \in (0,T], \tag{24}$$

for all $(u_{ep}, u_s, u_e) \in H^1_{\Gamma_{ep},0}(\Omega_{ep}) \times H^1(\Omega_s) \times H^1(\Omega_e)$, and

$$w_i'(0) = -p_{ex}'(0),\ w_i(0) = -p_{ex}(0) \text{ in } L^2(\Omega_i),\ i = ep, s, e. \tag{25}$$

Then $p_i = p_{ex} + w_{p_i}, i = ep, s, e$.

3. Stability for the drug concentration

The stability for the weak solution of the IBVP (1)-(6) defined by (16), (17) will be used now to conclude the stability of the weak solution of the IBVP (7)-(15).

The weak solution of the IBVP (7)-(15) that we study in what follows is defined by: $(c_{ep}, c_s, c_e) \in H^1([0,T], \prod_{i=ep,s,e} L^2(\Omega_i)) \cap L^2(0,T, \prod_{i=ep,s,e} H^1(\Omega_i))$ such that $c_{ep} = c_{\Gamma_{ep}}$ on $\Gamma_{ep} \times (0,T]$ and

$$\sum_{i=ep,s,e} \Big((c_i'(t), u_i)_{L^2(\Omega_i)} - (\mathbf{v}_i(t) c_i(t), \nabla u_i)_{[L^2(\Omega_i)]^2} + (D_i(t) \nabla c_i(t), \nabla u_i)_{[L^2(\Omega_i)]^2} \Big) = -(k_{ep,s}[c(t)], [u])_{L^2(\Gamma_{ep,s})} - (k_{s,e}[c(t)], [u])_{L^2(\Gamma_{s,e})} - (k_e c_e(t), u_e)_{L^2(\Gamma_e)}, \tag{26}$$

for all $(u_{ep}, u_s, u_e) \in H^1_{\Gamma_{ep},0}(\Omega_{ep}) \times H^1(\Omega_s) \times H^1(\Omega_e)$,$t \in (0,T]$, and

$$c_i(0) = 0 \text{ in } L^2(\Omega_i),\ i = ep, s, e. \tag{27}$$

In (26), $\mathbf{v}_i(t)$ denotes the convective velocity that we assume to be dependent on $p_i(t), \nabla p_i(t), i = ep, s, e$, $\mathbf{v}_i(t) = (v_{i,1}(t), v_{i,2}(t))$, with $v_{i,1}(t) = v_{i,1}(p_i(t), \frac{\partial p_i}{\partial x_1}(t))$ and $v_{i,2}(t) = v_{i,2}(p_i(t), \frac{\partial p_i}{\partial x_2}(t))$. Moreover, the following notations were used:

$$(k_{ep,s}[c(t)], [u])_{L^2(\Gamma_{ep,s})} = \int_{\Gamma_{ep,s}} k_{ep,s}[c(t)][u] d\mu$$

$$[c(t)] = c_{ep}(t) - c_s(t), [u] = u_{ep} - u_s \text{ on } \Gamma_{ep,s},$$

c_{ep}, c_s, u_{ep}, u_s on $\Gamma_{ep,s}$ are given by Trace Theorem (see for instance Theorem 1, pp. 272 of [5]). In (26), $(k_{s,e}[c(t)], [u])_{L^2(\Gamma_{s,e})}$ is defined analogously.

A common approach to solve the non homogeneous (26), (27) is to consider an extension c_{ex} of $c_{\Gamma_{ep}}$ to obtain a function in $H^1(\Omega)$. Then, $w_i(t) = c_i(t) - c_{ex}(t), i = ep, s, e$, are such that $w_{ep}(t) \in H^1_{\Gamma_{ep},0}(\Omega_{ep})$ and

$$\begin{aligned}
&\sum_{i=ep,s,e} \Big((w_i'(t), u_i)_{L^2(\Omega_i)} - (\mathbf{v}_i(t) w_i(t), \nabla u_i)_{[L^2(\Omega_i)]^2} + (D_i(t) \nabla w_i(t), \nabla u_i)_{[L^2(\Omega_i)]^2} \Big) \\
&+ (k_{ep,s}[w(t)], [u])_{L^2(\Gamma_{ep,s})} + (k_{s,e}[w(t)], [u])_{L^2(\Gamma_{s,e})} + (k_e w_e(t), u_e)_{L^2(\Gamma_e)} \\
&= \sum_{i=ep,s,e} \Big(- (c_{ex}'(t), u_i)_{L^2(\Omega_i)} + (\mathbf{v}_i(t) c_{ex}(t), \nabla u_i)_{[L^2(\Omega_i)]^2} - (D_i \nabla c_{ex}(t), \nabla u_i)_{[L^2(\Omega_i)]^2} \Big) \\
&- (k_{ep,s}[c_{ex}(t)], [u])_{L^2(\Gamma_{ep,s})} - (k_{s,e}[c_{ex}(t)], [u])_{L^2(\Gamma_{s,e})} - (k_e c_{ex}(t), u_e)_{L^2(\Gamma_e)},
\end{aligned} \tag{28}$$

for all $(u_{ep}, u_s, u_e) \in H^1_{\Gamma_{ep,0}}(\Omega_{ep}) \times H^1(\Omega_s) \times H^1(\Omega_e)$, for all $t \in (0, T]$, and

$$w_i(0) = -c_{ex}(0) \text{ in } L^2(\Omega_i),\ i = ep, s, e. \tag{29}$$

Then, $c_i(t) = w_i(t) + c_{ex}(t), t \in [0, T],\ i = ep, s, e$.

In what follows we present the main stability result. To simplify the presentation we take $k_{ep,s} = k_{s,e} = 1$.

Proposition 2. *Let (p_{ep}, p_s, p_e) and $(\tilde{p}_{ep}, \tilde{p}_s, \tilde{p}_e)$ be solutions of the IBVP (16), (17) belonging to $L^2([0, T], \prod_{i=ep,s,e} H^1(\Omega_i))$ and let $(c_{ep}, c_s, c_e), (\tilde{c}_{ep}, \tilde{c}_s, \tilde{c}_e) \in C^1(0, T, \prod_{i=ep,s,e} L^2(\Omega_i)) \cap L^2(0, T, \prod_{i=ep,s,e} H^1(\Omega_i))$ be the corresponding solutions of differential problem (26), (27) where $(\tilde{c}_{ep}, \tilde{c}_s, \tilde{c}_e)$ satisfies the initial condition*

$$\tilde{c}_i(0) = \tilde{c}_{inc,i} \ \text{ in } L^2(\Omega_i), i = ep, s, e. \tag{30}$$

If $D_i(t) \geq D_{i,0} > 0$ in $\mathbb{R} \times [0, T], i = ep, s, e$, D_i, $\mathbf{v}$ and k_e are Lipschitz functions with Lipschitz constants L_D, L_v and L_k, respectively.

Let $\omega_{p,i} = p_i - \tilde{p}_i$ and $\omega_{c,i} = c_i - \tilde{c}_i, i = ep, s, e$. Then there exists a positive constant $C_{s,c}$, $p, \tilde{p}, c, \tilde{c}$ independent, such that

$$\begin{aligned}
&\sum_{i=ep,s,e} \Big(\|\omega_{c,i}(t)\|^2_{L^2(\Omega_i)} + \int_0^t e^{\int_s^t g(\mu)d\mu} \|\nabla\omega_{c,i}(s)\|^2_{[L^2(\Omega_i)]^2} ds \Big) \\
&+ \int_0^t e^{\int_s^t g(\mu)d\mu} \Big(\|\omega_{c,e}(s)\|^2_{L^2(\Gamma_e)} + \|[\omega_c(s)]\|^2_{L^2(\Gamma_{ep,s}\cup\Gamma_{s,e})} \Big) ds \\
&\leq C_{s,c} \Big(\sum_{i=ep,s,e} e^{\int_0^t g(\mu)d\mu} \|\tilde{c}_{inc,i}\|^2_{L^2(\Omega_i)} + \int_0^t e^{\int_s^t g(\mu)d\mu} \pi(\omega_p(s), \nabla\omega_p(s)) ds \Big),
\end{aligned} \tag{31}$$

with

$$g(\mu) = \max_{i=ep,s,e} \|\tilde{\mathbf{v}}_i(\mu)\|_{\infty, L^\infty(\Omega_i)} = \max_{i=ep,s,e} \max_{j=1,2} \|v_{i,j}(\tilde{p}_i(\mu), \frac{\partial \tilde{p}_i}{\partial x_j}(\mu))\|_{L^\infty(\Omega_i)}$$

and

$$\begin{aligned}
\pi(\omega_p(t), \nabla\omega_p(t)) \;=\; &\sum_{i=ep,s,e} \|\omega_{p,i}(t)\|^2_{H^1(\Omega_i)} \|c_i(t)\|^2_{L^\infty(\Omega_i)} \\
&+ \|\omega_{p,i}(t)\|^2_{L^\infty(\Omega_i)} \|\nabla c_i(t)\|^2_{[L^2(\Omega_i)]^2} \Big) \\
&+ \|\omega_{p,e}(t)\|^2_{L^\infty(\Gamma_e)} \|c_e(t)\|^2_{L^2(\Gamma_e)}
\end{aligned} \tag{32}$$

Proof: From (26), for $\omega_p(t)$ and $\omega_c(t)$ we deduce the following

$$\begin{aligned}
\sum_{i=ep,s,e} (\omega'_{c,i}(t), \omega_{c,i}(t))_{L^2(\Omega_i)} \;&= -((k_e(p_e(t)) - k_e(\tilde{p}_e(t)))c_e(t), \omega_{c,e}(t))_{L^2(\Gamma_e)} \\
&\quad -(k_e(\tilde{p}_e(t)))\omega_{c,e}(t), \omega_{c,e}(t))_{L^2(\Gamma_e)} \\
&\quad -\|[\omega_c(t)]\|^2_{L^2(\Gamma_{ep,s}\cup\Gamma_{s,e})} + \sum_{j=1}^{4} S_j,
\end{aligned} \tag{33}$$

with

$$S_1 = \sum_{i=ep,s,e} (\mathbf{v}_i(p_i(t), \nabla p_i(t)) - \mathbf{v_i}(\tilde{p}_i(t), \nabla\tilde{p}_i(t))c_i(t), \nabla\omega_{c,i}(t))_{[L^2(\Omega_i)]^2},$$

$$S_2 = \sum_{i=ep,s,e} (\mathbf{v}_i(\tilde{p}_i(t), \nabla\tilde{p}_i(t))\omega_{c,i}(t), \nabla\omega_{c,i}(t))_{[L^2(\Omega_i)]^2},$$

$$S_3 = -\sum_{i=ep,s,e} ((D_i(p_i(t)) - D_i(\tilde{p}_i(t)))\nabla c_i(t), \nabla\omega_{c,i}(t))_{[L^2(\Omega_i)]^2}$$

and

$$S_4 = -\sum_{i=ep,s,e} (D_i(\tilde{p}_i(t)))\nabla\omega_{c,i}(t), \nabla\omega_{c,i}(t))_{[L^2(\Omega_i)]^2}.$$

As $\mathbf{v}$ is a Lipschitz function with Lipschitz constant L_v for S_1 we get

$$|S_1| \leq \sum_{i=ep,s,e} \Big(\frac{1}{2\epsilon_i^2} L_v^2 \big(\|\omega_{p,i}(t)\|^2_{L^2(\Omega_i)} + \|\nabla\omega_{p,i}(t)\|^2_{[L^2(\Omega_i)]^2}\big)\|c_i(t)\|^2_{L^\infty(\Omega_i)} + \epsilon_i^2\|\nabla\omega_{c,i}(t)\|^2_{[L^2(\Omega_i)]^2}\Big), \tag{34}$$

where $\epsilon_i \neq 0, i = ep, s, e$, are arbitrary constants.

For S_2 we easily obtain

$$|S_2| \leq \sum_{i=ep,s,e} \frac{1}{4\beta_i^2}\|\tilde{\mathbf{v}}_i(t)\|^2_{\infty,L^\infty(\Omega_i)}\|\omega_{c,i}(t)\|^2_{L^2(\Omega_i)} + \beta_i^2\|\nabla\omega_{c,i}(t)\|^2_{[L^2(\Omega_i)]^2}, \tag{35}$$

where $\beta_i \neq 0, i = ep, s, e$, are arbitrary constants.

Considering that $D_i, i = ep, s, e$, are also a Lipschitz functions we deduce

$$|S_3| \leq \sum_{i=ep,s,e} \frac{1}{4\gamma_i^2} L_D^2\|\omega_{p,i}(t)\|^2_{L^\infty(\Omega_i)}\|\nabla c_i(t)\|^2_{[L^2(\Omega_i)]^2} + \gamma_i^2\|\nabla\omega_{c,i}(t)\|^2_{[L^2(\Omega_i)]^2}, \tag{36}$$

where $\gamma_i \neq 0, i = ep, s, e$, are arbitrary constants.

Finally, we also have

$$\begin{aligned} &-((k_e(p_e(t)) - k_e(\tilde{p}_e(t)))c_e(t), \omega_{c,e}(t))_{L^2(\Gamma_e)} - (k_e(\tilde{p}_e(t)))\omega_{c,e}(t), \omega_{c,e}(t))_{L^2(\Gamma_e)} \\ &\quad \leq \frac{1}{4\alpha^2} L_k^2\|\omega_{p,e}(t)\|^2_{L^\infty(\Gamma_e)}\|c_e(t)\|^2_{L^2(\Gamma_e)} + \alpha^2\|\omega_{c,e}(t)\|^2_{L^2(\Gamma_e)} - \|\sqrt{k_e}\omega_{c,e}(t)\|^2_{L^2(\Gamma_e)}, \end{aligned} \tag{37}$$

where $\alpha \neq 0$ is an arbitrary constant, and

$$S_4 \geq -\sum_{i=ep,s,e} D_{i,0}\|\nabla\omega_{c,i}(t)\|^2_{[L^2(\Omega_i)]^2}. \tag{38}$$

Inserting the bounds (34)-(38) in (33) we establish

$$\begin{aligned}\frac{1}{2}\frac{d}{dt}\sum_{i=ep,s,e}\|\omega_{c,i}(t)\|^2_{L^2(\Omega_i)}+\sum_{i=ep,s,e}(D_{i,0}-\beta_i^2-\epsilon_i^2-\gamma_i^2)\|\nabla\omega_{c,i}(t)\|^2_{[L^2(\Omega_i)]^2}\\ +\|\sqrt{k_e}\omega_{c,e}(t)\|^2_{L^2(\Gamma_e)}-\alpha^2\|\omega_{c,e}(t)\|^2_{L^2(\Gamma_e)}+\|[\omega_c(t)]\|^2_{L^2(\Gamma_{ep,s}\cup\Gamma_{s,e})}\\ \leq\sum_{i=ep,s,e}\frac{1}{4\beta_i^2}\|\tilde{\mathbf{v}}_i(t)\|^2_{\infty,L^\infty(\Omega_i)}\|\omega_{c,i}(t)\|^2_{L^2(\Omega_i)}+\hat{\pi}(\omega_p(t),\nabla\omega_p(t)),\end{aligned}\tag{39}$$

with

$$\begin{aligned}\hat{\pi}(\omega_p(t),\nabla\omega_p(t))=\sum_{i=ep,s,e}\Big(\frac{1}{2\epsilon_i^2}L_v^2\Big(\|\omega_{p,i}(t)\|^2_{L^2(\Omega_i)}+\|\nabla\omega_{p,i}(t)\|^2_{[L^2(\Omega_i)]^2}\Big)\|c_i(t)\|^2_{L^\infty(\Omega_i)}\\ +\tfrac{1}{4\gamma_i^2}L_D^2\|\omega_{p,i}(t)\|^2_{L^\infty(\Omega_i)}\|\nabla c_i(t)\|^2_{[L^2(\Omega_i)]^2}\Big)\\ +\tfrac{1}{4\alpha^2}L_k^2\|\omega_{p,e}(t)\|^2_{L^\infty(\Gamma_e)}\|c_e(t)\|^2_{L^2(\Gamma_e)}.\end{aligned}$$

From (39), fixing conveniently the arbitrary constants $\beta_i, \epsilon_i, \gamma_i, i = ep, s, e$, and α, we easily guarantee the existence of a positive constant $C_{s,c}$ satisfying (31) with $\pi(\omega_p(t), \nabla\omega_p(t))$ defined by (32).

■

We remark the following:

(1) If (p_{ep}, p_s, p_e) and $(\tilde{p}_{ep}, \tilde{p}_s, \tilde{p}_e)$ are solutions of the IBVP (16), (17) in

$$C^2([0,T],\prod_{i=ep,s,e}L^2(\Omega_i))\cap C^1([0,T],\prod_{i=ep,s,e}H^1(\Omega_i))\cap C([0,T],\prod_{i=ep,s,e}H^2(\Omega_i)),$$

by Corollary 1 of Proposition 1, an upper bound for $\pi(\omega_p(t), \nabla\omega_p(t))$ is established.

(2) We observe that the coupled problem (16), (17), (26), (27) is nonlinear in the acoustic pressure $p_i, i = ep, s, e$. Consequently, the stability holds locally. The stability of the coupled problem (16), (17), (26), (27) is consequence of Propositions 1 and 2.

(3) To guarantee the stability of the coupled problem (16), (17), (26), (27) in p and c satisfying the assumptions of Propositions 1 and 2, we need to impose that

$$\int_0^T\|c_i(\mu)\|^2_{L^\infty(\Omega_i)}d\mu\leq C,\int_0^T\|\nabla c_i(\mu)\|^2_{[L^2(\Omega_i)]^2}d\mu\leq C, i=ep,s,e,$$

$$\int_0^T \|c_e(\mu)\|^2_{L^2(\Gamma_e)} d\mu \leq C.$$

(4) if $v_{i,j}$, $j = 1, 2$, $i = ep, s, e$, are bounded in $\mathbb{R}^2$, then there exists a positive constant C, $p, \tilde{p}, c, \tilde{c}$ independent, such that $\|\tilde{\mathbf{v}}(\mu)\|_{\infty, L^\infty(\Omega_i)} \leq C, i = ep, s, e$, and the stability follows.

4. Numerical simulation

4.1. Piecewise linear finite element approximations for the acoustic pressure and concentration. In what follows we assume that the boundaries of $\Omega_i, i = ep, s, e$, are polygonal lines. Let $\mathcal{T}_{i,h}, i = ep, s, e$, be a sequence of admissible triangulations of $\Omega_i, i = ep, s, e$, respectively, with $\max_{\Delta \in \mathcal{T}_{i,h}} diam(\Delta) \to 0, i = ep, s, e$. We assume that $\mathcal{T}_{ep,h}$ and $\mathcal{T}_{s,h}$ are compatible with respect to $\Gamma_{ep,s}$ in the following sense: if $\Delta_1 \in \mathcal{T}_{ep,h}$ and $\Delta_2 \in \mathcal{T}_{s,h}$ are such that $\bar{\Delta}_1 \cap \bar{\Delta}_2 \neq \emptyset$ and $\bar{\Delta}_1 \cap \Gamma_{ep,s} \neq \emptyset$, $\bar{\Delta}_2 \cap \Gamma_{ep,s} \neq \emptyset$, then $\bar{\Delta}_1 \cap \bar{\Delta}_2$ is the common side of these two triangles that is contained in $\Gamma_{ep,s}$. We also assume that $\mathcal{T}_{s,h}$ and $\mathcal{T}_{e,h}$ are compatible with respect to $\Gamma_{s,e}$.

Let P_h be the piecewise linear interpolator operator. By $V_{i,h}$ we denote the subspace of $H^1(\Omega_i)$ defined by the piecewise linear functions u_h induced by the triangulation $\mathcal{T}_{i,h}$ for $i = ep, s, e$.

By $(p_{ep,h}(t), p_{s,h}(t), p_{e,h}(t)) \in \prod_{i=ep,s,e} V_{i,h}$ we denote the piecewise linear approximation for the solution of the IVP (16), (17) defined by: $p_{ep,h}(t) = p_{h,\Gamma_{ep}}(t)$ on $\Gamma_{ep} \times (0, T]$ and

$$\sum_{i=ep,s,e} \left((p''_{i,h}(t), u_{i,h})_{L^2(\Omega_i)} + \nu_i (\nabla p_{i,h}(t), \nabla u_{i,h})_{[L^2(\Omega_i)]^2} \right) = 0, \; t \in (0, T], \quad (40)$$

for all $(u_{ep,h}, u_{s,h}, u_{e,h}) \in V^{(0)}_{ep,h} \times V_{s,h} \times V_{e,h}$, and

$$p'_{i,h}(0) = 0 = p_{i,h}(0) = 0 \text{ in } L^2(\Omega_i), i = ep, s, e. \quad (41)$$

In the definition of the piecewise linear approximation for the pressure, $V^{(0)}_{ep,h} = \{u_h \in V_{ep,h} : u_h = 0 \text{ on } \Gamma_{ep}\}$ and $p_{\Gamma_{ep},h}(t)$ is the piecewise linear interpolator of $p_{\Gamma_{ep}}(t)$.

Let us consider now the piecewise linear finite element for the concentration that we introduce in what follows. Let $(c_{ep,h}(t), c_{s,h}(t), c_{e,h}(t)) \in \prod_{i=ep,s,e} V_{i,h}$

be such that $c_{ep}(t) = c_{\Gamma_{ep},h}(t)$ on Γ_{ep} and

$$\begin{aligned}\sum_{i=ep,s,e}(\frac{\partial c_{i,h}}{\partial t}(t), u_{i,h})_{L^2(\Omega_i)} + \sum_{i=ep,s,e}(D_i(t)\nabla c_{i,h}(t), \nabla u_{i,h})_{[L^2(\Omega_i)]^2}\\ = \sum_{i=ep,s,e}(\mathbf{v}_{i,h}(t)c_{i,h}(t), \nabla u_{i,h})_{[L^2(\Omega_i)]^2}\\ -(k_{ep,s}[c_h(t)], [u_h])_{L^2(\Gamma_{ep,s})} - (k_{s,e}[c_h(t)], [u_h])_{L^2(\Gamma_{s,e})}\\ -(k_e c_{e,h}(t), u_{e,h})_{L^2(\Gamma_e)}, t \in (0,T],\end{aligned} \tag{42}$$

for all $(u_{ep,h}, u_{s,h}, u_{e,h}) \in V^{(0)}_{ep,h} \times V_{s,h} \times V_{e,h}$, and

$$c_{i,h}(0) = 0 \text{ in } L^2(\Omega_i),\ i = ep, s, e. \tag{43}$$

In (42), $\mathbf{v}_{i,h} = (v_{i,1}(p_{i,h}(t), \nabla p_{i,h}(t)), v_{i,2}(p_{i,h}(t), \nabla p_{i,h}(t)))$, with $p_{i,h}(t), i = ep, s, e$, given by (40), (41), $c_{\Gamma_{ep,h}}(t)$ is the piecewise linear interpolator of $c_{\Gamma_{ep}}(t)$ on Γ_{ep}, and $[c_h(t)] = c_{ep,h}(t) - c_{s,h}(t)$ on $\Gamma_{ep,s}$ and $[c_h(t)] = c_{s,h}(t) - c_{e,h}(t)$ on $\Gamma_{s,e}$ for $t \in (0,T]$, $[u_h(t)]$ on $\Gamma_{ep,s}$ and on $\Gamma_{s,e}$ is defined analogously.

The stability analysis for the IVP (40), (41), (42) and (43) can be stated following the proof of Proposition 1 and its corollary 1 and Proposition 2. In fact, these results can be established for the IVP (40), (41), (42) and (43) where the corresponding upper bounds depend on the finite element approximations. For instance, the stability upper bound (31) holds for the finite element solutions $p_{ep,h}(t), \tilde{p}_{ep,h}(t), c_{i,h}(t), \tilde{c}_{i,h}(t), i = ep, s, e$, defined by (40), (41), (42) and (43). To guarantee the stability of the coupled finite element method, we should guarantee that the second member of the inequality (31) in finite element context is bounded, that is, the term corresponding to (32) defined by

$$\begin{aligned}\hat{\pi}(\omega_{p_h}(t), \nabla\omega_{p_h}(t)) = \sum_{i=ep,s,e}\Big(&\|\omega_{p_h,i}(t)\|^2_{H^1(\Omega_i)}\|c_{i,h}(t)\|^2_{L^\infty(\Omega_i)}\\ &+\|\omega_{p_h,i}(t)\|^2_{L^\infty(\Omega_i)}\|\nabla c_{i,h}(t)\|^2_{[L^2(\Omega_i)]^2}\Big)\\ &+\|\omega_{p_h,e}(t)\|^2_{L^\infty(\Gamma_e)}\|c_{e,h}(t)\|^2_{L^2(\Gamma_e)}\Big),\end{aligned} \tag{44}$$

is bounded. In (44), $\omega_{p,i}(t) = p_{i,h} - \tilde{p}_{i,h}(t), i = ep, s, e$.

Let us consider a simplified version of our model defined considering the cornea as a unique domain Ω. Let $\mathcal{T}_h$ be a quasi-uniform triangulation of Ω and let S_h be the space of continuous functions in $\overline{\Omega}$ which are linear in each triangle of $\mathcal{T}_h$ and null on Γ_{ep}. To obtain the stability of the corresponding

Diameter of $\mathcal{T}_{i,h}, i = eps, s, e$	Error in epithelium	Error in endothelium.
0.01	5.81813×10^{-5}	1.11626×10^{-6}
0.0067	4.36563×10^{-5}	9.3682×10^{-7}
0.0034	3.87258×10^{-5}	8.5983×10^{-7}

TABLE 1. Errors (L^∞) for concentration in epithelium and endothelium.

Diameter of $\mathcal{T}_{i,h}, i = eps, s, e$	Error in epithelium	Error in endothelium.
0.01	0.022579	0.003752
0.0067	0.013645	0.002395
0.0034	0.011248	0.001853

TABLE 2. Errors (L^2) for concentration in epithelium and endothelium.

Diameter of $\mathcal{T}_{i,h}, i = eps, s, e$	Error in epithelium	Error in endothelium.
0.01	0.026351	0.003756
0.0067	0.023608	0.003753
0.0034	0.023047	0.003746

TABLE 3. Errors (H^1) for concentration in epithelium and endothelium.

finite element approximation, it is necessary to obtain upper bounds for the errors $\|p(t) - p_h(t)\|_{H^1(\Omega)}$ as well as for $\|p(t) - p_h(t)\|_{L^\infty(\Omega)}$ and $\|p(t) - p_h(t)\|_{L^\infty(\Gamma_e}$, $\|c(t) - c_h(t)\|^2_{L^\infty(\Omega)}$ and $\|c(t) - c_h(t)\|^2_{L^2(\Gamma_e)}$. The establishment of upper bounds for the last errors even in the simplified version need to be investigated.

4.2. Numerical Results. The numerical results presented in what follows were obtained using the commercial tool COMSOL 5.3 Multiphysics. Piecewise linear finite element space P_1 for the concentration and pressure is used and backward differential formulae with orders between 1 and 2 with a time-step equal to $0.1s$ are used to integrate in time.

In what follows we consider the computational mesh illustrated in Figure 3. The adequacy of the mesh has been investigated using convergence tests considering different meshes and a reference solution computed with $h_{max} = 10^{-4}$. The results included in Tables 1, 2 and 3 are computed considering the maximum in time of the indicated norm of the difference between the reference solution and the solutions obtained with the triangular meshes with the indicated h_{max}. Taking into account these results we conclude that the numerical results are not sensitive with respect to the meshes used.

The parameters and the corresponding values used in what follows are given in Tables 4 and 5.

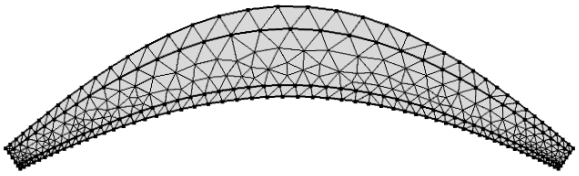

FIGURE 3. Computational mesh.

Symbol	Numerical value			Refs.
	Epithelium	Stroma	Endothelium	
$D_{j_0}(j = ep, s, e)$	6.71×10^{-10}	6.1×10^{-10}	11.1×10^{-10}	[2]
$A_j(j = ep, s, e)$	10^{-4}	9.8×10^{-5}	7.2×10^{-5}	[2]
c_{la}	7.344×10^{-6}	4.678×10^{-5}	7.8291×10^{-5}	[2]

TABLE 4. Values of the parameters, diffusion coefficient (m^2/s), surface area (m^2) and clearance rate$(1/s)$, used in the numerical experiments.

Symbol	Definition	Numerical value	Refs.
$\nu_j(j = ep, s, e)$	Material sound speed$((m/s)^2)$	2	[7]
$\phi_{j_0}(j = ep, s, e)$	Porosity at a reference pressure	0.25	[3]
$\beta_{j_0}(j = ep, s, e)$	Normalization constant	10^{-8}	[3]
$\mathcal{K}$	Kozeny coefficient$(1/s)$	2	[10]
$\tau_j(j = ep, s, e)$	Tortuosity of the medium(m/s)	1	[10]
μ	Viscosity of the medium$(kg/m.s)$	10^{-3}	[3]
c_R	Reservoir concentration(mol/m^3)	1	-
$k_{i,j}$	Mass transfer coefficient(m/s)	10^{-4}	-
$p_{\Gamma_{ep}}$	Acoustic pressure on Γ_{ep} (Pa)	1	-

TABLE 5. Values of the other parameters used in the numerical experiments.

In Figure 4 we illustrate, qualitatively, the effect of the ultrasound on the drug transport. In the left figure we present the mean drug concentration in the stroma with and without ultrasound. In the right figure we plot the corresponding drug mass in the anterior chamber. We observe that the pressure waves generated by the ultrasound increase the drug concentration in the cornea and, consequently, the drug mass that will be available in the anterior chamber also increases. These figures clearly illustrate the effect of ultrasound on drug transport through the cornea.

In Table 6 we include the average drug concentration in the stroma and in the anterior chamber for different times. From these results, we conclude

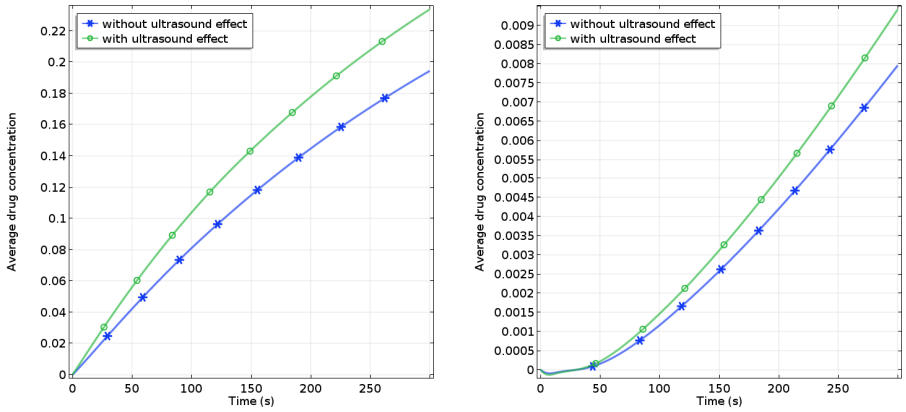

(a) *Stroma* (b) *Anterior chamber*

FIGURE 4. Time evolution of the average drug concentration in the stroma ((a)) and of the drug mass in the anterior chamber ((b)) for $t = 300s$.

	stroma		*anterior chamber*	
time(s)				
	with	*without*	*with*	*without*
0	6.0995×10^{-9}	5.9031×10^{-9}	1.7530×10^{-13}	1.7521×10^{-13}
60	0.066164	0.050252	4.0825×10^{-4}	3.0068×10^{-4}
120	0.12066	0.094975	0.0020851	0.0017001
180	0.16462	0.13314	0.0042347	0.0035270
240	0.20195	0.16595	0.0067024	0.0056381
300	0.23370	0.19434	0.0094189	0.0079541

TABLE 6. Average drug concentration in stroma and in anterior chamber for different times.

that as time increases, the drug concentration increases in both corneal compartments being the drug concentration enhanced by ultrasound greater than the drug concentration without the enhancer.

The drug transport enhanced by ultrasound has two main contributions: a Fickian transport and a convective transport. To illustrate the importance of the convection generated by ultrasound, in Figure 5 we plot the average drug concentrations in the stroma and in the anterior chamber computed with and without the convective transport. From these plots, we conclude that the convective field induced by ultrasound has an important role in the drug transport.

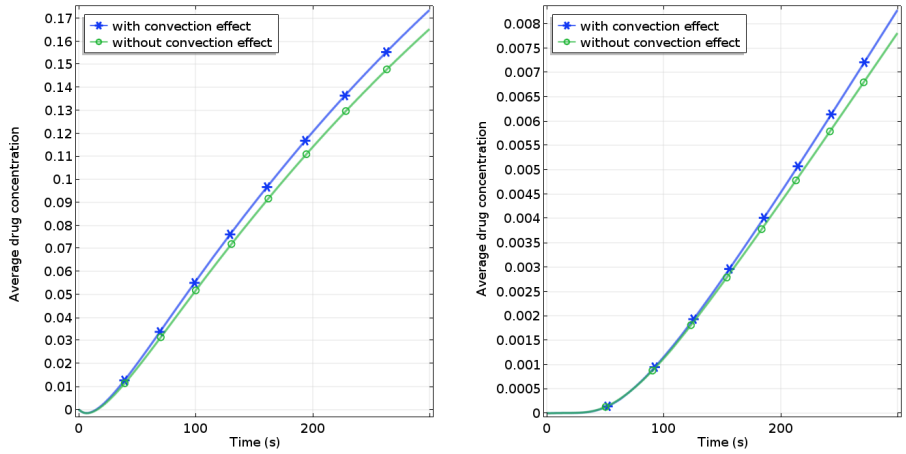

(a) *Stroma* (b) *Anterior chamber*

FIGURE 5. Time evolution of the average drug concentration with and without the convective transport induced by ultrasound in the stroma ((a)) and in the anterior chamber ((b)) for $t = 300s$.

Figure 7 illustrates the behaviour of the drug concentration in each corneal layer when the mass transfer coefficient $k_{ep,s}$ between the epithelium and the stroma changes. As this parameter increases, decreases the drug concentration in the epithelium and increases the drug concentration in the stroma and endothelium. In fact, the promotion of the drug transport through $\Gamma_{ep,s}$ is mathematically translated by the increasing of $k_{ep,s}$ that leads to an increasing of the drug concentration in the stroma and endothelium and a decreasing in the epithelium.

To conclude this section devoted to the illustration of the qualitative behaviour of the drug concentration in the corneal layers when the drug transport through the cornea is enhanced by ultrasound, we present a comparison between numerical results and experimental data obtained from [6]. In this paper, experiments involving the transport of sodium fluorescein through rabbit corneas enhanced by ultrasound are presented. The results were obtained by exposing the cornea to pressure waves generated from a $800kHz$ transducer and intensity equal to 2 W/cm^2 during 5 minutes.

In Figure 8 we compare experimental data with simulation results, where the experimental data are taken from [6] considering the initial time coinciding with $t = 10^3 s$. We observe a good agrement between both results which shows the potential of the mathematical model (40), (41), (42) and (43) to describe the drug transport in the cornea enhanced by ultrasound.

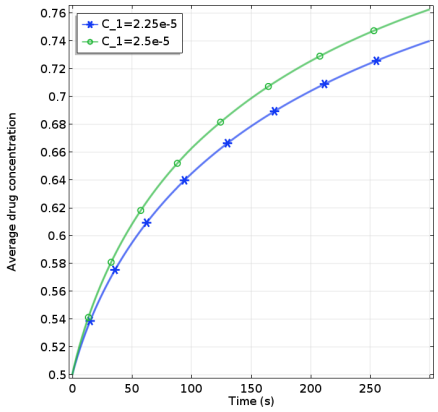

(a) *Epithelium*

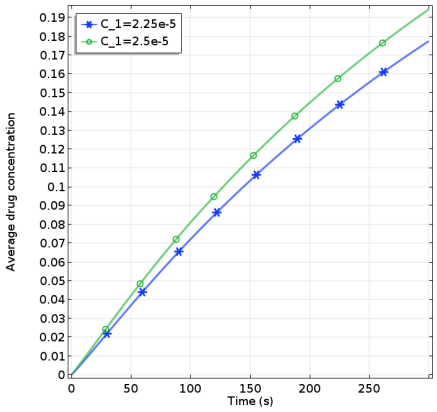

(b) *Stroma*

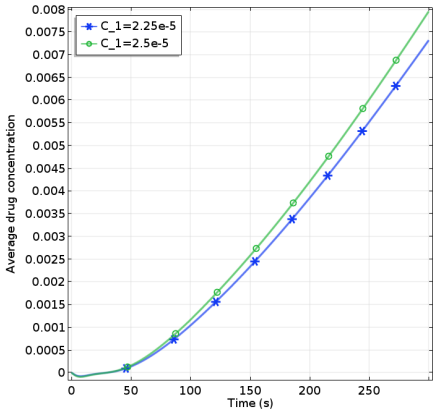

(c) *Endothelium*

FIGURE 6. Time evolution of the average drug concentration in the epithelium ((a)), stroma ((b)) and endothelium ((c)) for different wave propagation speeds in the epithelium.

5. Conclusions

The human eye is a fortress that has a diverse set of defenses that protects it from surrounding environment. In what concerns the anterior part of the eye, these defenses include, among others, the reflex blinking, the tear film (thin transparent fluid layer) and the tear fluid turnover, the nasolacrimal drainage system as well as the lower permeability of the cornea. When an eye drop is instilled in the eye, the defense system is responsible by the loss of a significant amount of drug. Consequently, only 5% of the applied drug reaches the intraocular tissue.

In the present paper we study, from mathematical and simulation point of views, the role of pressure waves generated by ultrasound as enhancer

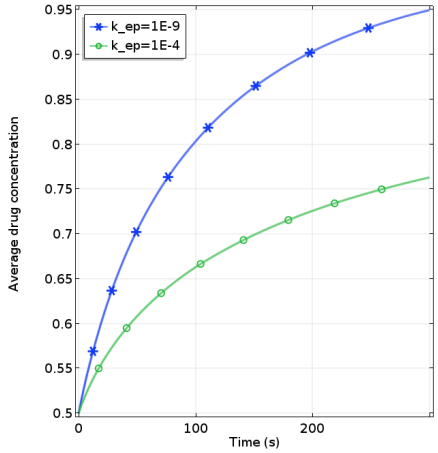

(a) *Epithelium*

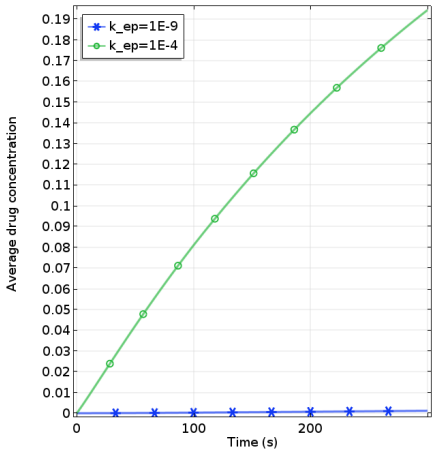

(b) *Stroma*

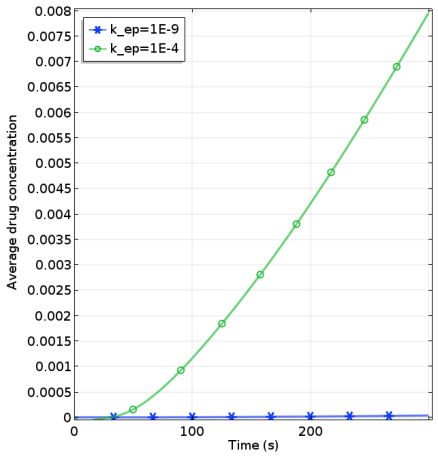

(c) *Endothelium*

FIGURE 7. Time evolution of the average drug concentration in the three corneal layers: epithelium ((a)), stroma ((b)) and endothelium ((c)) for different values of the mass transfer coefficient $k_{ep,s}$.

to increase the drug transport through the corneal layers. The ultrasound generates pressure waves that increase the porosity of the cornea and, consequently, increase the diffusive and convective drug transports. In fact, the diffusion coefficients and permeability of the corneal layers depend on the porosity and by Darcy's law, the convective velocity also depends on the pressure waves intensity.

At the best of our knowledge, this is the first study on this subject - mathematical modeling of the coupling between pressure waves generated

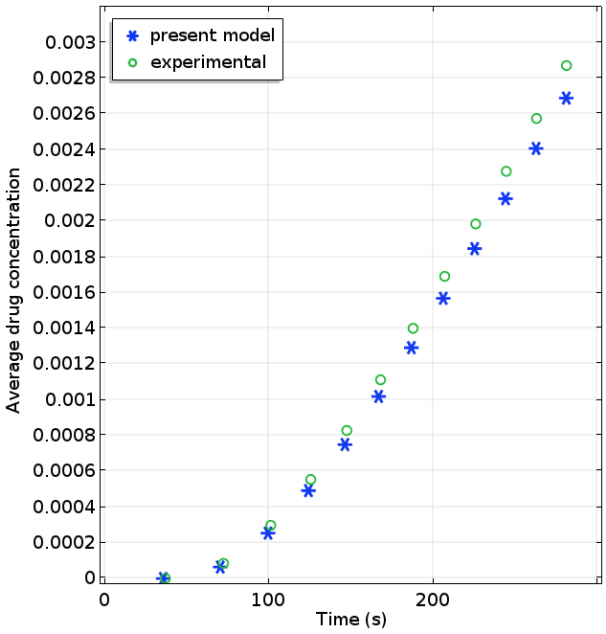

FIGURE 8. Experimental data from [6] and average drug concentration that reaches the anterior chamber obtained from the model.

by ultrasound and the drug transport through to the corneal layers considering the dependence of the diffusion coefficient and the convective velocity on the porosity induced by the propagation of pressure waves generated by ultrasound.

From the numerical experiments presented in the last section, the following conclusions can be stated:

- An increasing in the acoustic pressure on the boundary Γ_{ep} leads to an increasing of the drug concentration in the corneal layers and an increasing of the drug that reaches the anterior chamber (Figure 4 and Table 6);
- The pressure waves induce a convective flow in the corneal layers and, consequently, lead to an increasing of the drug concentration in the corneal layers (Figure 5);
- An increasing in the waves propagation speed in the epithelium leads to an increasing on the porosity and permeability of the different corneal layers. Consequently, also lead to a decreasing of the drug concentration in the first layer and an increasing of the drug concentration in the two last corneal layers (Figure 6).

From theoretical point of view, the stability of the coupled problem (16), (17), (26), (27) is established in Propositions 1 and 2. Similar results hold for the semi-discrete approximation defined by piecewise linear finite element approximations for the acoustic pressure and for the concentration.

Acknowledgments

This work was partially supported by the Centre for Mathematics of the University of Coimbra - UIDB/00324/2020, funded by the Portuguese Government through FCT/MCTES.

References

[1] H. Almogbil, F. Montecinos-Franjola, C. Daszynski, W. Conlon, J. Hachey, G. Corazza, E. Rodriguez, V. Zderic, *Therapeutic ultrasound for topical corneal delivery of macromolecules*, Translational Vision Science and Technology, 11 (2022), 23.

[2] R. Avtar, D. Tandon, *Modeling the drug transport in the anterior segment of the eye*, European journal of pharmaceutical sciences, 35 (2008), 175-182.

[3] D. T. Birdsell, S. Karra, H. Rajaram, *On the Representation of the Porosity-Pressure Relationship in General Subsurface Flow Codes*, Water Resources Research, 54 (2018), 1382-1388.

[4] S. Chen, M. Mienaltowskia, D. Birk, *Regulation of corneal stroma extracellular matrix assembly*, Experimental Eye Research, 133 (2015), 69-80.

[5] L. Evans, *Partial Differential Equations*, American Mathematical Society, Providence, Rhode Island, Secon Edition, 2010.

[6] P. Hariharan, M. Nabili, A. Guan, V. Zderic, and M. Myers, *A model for porosity changes occurring during ultrasound-enhanced transcorneal drug delivery*, Ultrasound in Medicine and Biology, 43 (2017), 1223–1236.

[7] J.A. Ferreira, D. Jordão, L. Pinto, *Approximating coupled hyperbolic-parabolic systems arising in enhanced drug delivery*, Computers and Mathematics with Applications, 76 (2018), 81-97.

[8] U. Jegal, J.H. Lee, J. Lee, H. Jeong, M. J. Kim, K. H. Kim, *Ultrasound-assisted gatifloxacin delivery in mouse cornea, in vivo*, Scientific Reports, 9 (2019), 15532 .

[9] C. Jumellea, S. Gholizadehb, N. Annabib, R. Danaa, *Advances and limitations of drug delivery systems formulated as eye drops*, Journal of Controlled Release, 321 (2020), 1-22.

[10] A. Koponen, M. Kataja, and J. Timonen, *Permeability and effective porosity of porous media*, Physical Review E, 56 (1997), 3319–3325.

[11] K. Kooiman, S. Roovers, S. Langeveld, R. Kleven, H. Dewitte, M. O'Relly, J-M. Escoffre, A. Bouakaz, M. Verweij, K. Hynynen, I. Lentacker, E. Stride, C. Holland, *Ultrasound-responsive cavitation nuclei for therapy and drug delivery*, Ultrasound in Medicine and Biology, 46 (2020), 1296-1325.

[12] A. Ledesma-Durán, S. I. Hernández, and I. Santamaría-Holek, *Relation between the porosity and tortuosity of a membrane formed by disconnected irregular pores and the spatial diffusion coefficient of the Fick-Jacobs model*, Physical Review E, 95 (2017), 052804.

[13] S. Mahnič-Kalamiza, D. Miklavčič, E. Vorobieva, *Dual-porosity model of solute diffusion in biological tissue modified by electroporation*, Biochimica et Biophysica Acta (BBA) - Biomembranes, 1838 (2014), 1950–1966.

[14] M. Nabili, H. Patel, S. P. Mahesh, J. Liu, C. Geist, V. Zderic, *Ultrasound-enhanced delivery of antibiotics and anti-inflammatory drugs into the eye*, Ultrasound in Medicine and Biology, 39(2013), 638–6546.

[15] M. Nabili1, A. Shenoy, S. Chawla, S. Mahesh, J. Liu, C. Geist, V. Zderic, *Ultrasound-enhanced ocular delivery of dexamethasone sodium phosphate: an in vivo study*, Journal of Therapeutic Ultrasound, 2 (2014), 6.

[16] M. Nabili1, C. Geist, V. Zderic, *Thermal safety of ultrasound-enhanced ocular drug delivery - a modeling study*, Medical Physics, 42 (2015), 5604-5615.

[17] W. Pitt, G. Husseini, B. Staples, *Ultrasonic drug delivery - a general review*, Expert Opinion on Drug Delivery, 1(2004), 37-56.

[18] M. Rezaeiana, A. Sedaghatkishb, M. Soltani, *Numerical modeling of high-intensity focused ultrasound-mediated intraperitoneal delivery of thermosensitive liposomal doxorubicin for cancer chemotherapy*, Drug Delivery, 26 (2019), 898-917.

[19] C. Wang, F. Li, H. Li, *Gene therapy for ocular diseases mediated by ultrasound and microbubbles (Review)*, Molecular Medicine Reports, 12 (2015), 4803–4814.

[20] M. Wang, M. Li, P. Yan, Q. Luo, Y. Zhang, Z. Du, *The effect of high intensity focused ultrasound keratoplasty on rabbit anterior segment*, Journal of Ophthalmology, 2017 (2017), 6067890.

[21] W. Zhan1, W. Gedroy, X. Xu, *Towards a multiphysics modelling frameworkfor thermosensitive liposomal drug delivery to solid tumourcombined with focused ultrasound hyperthermia*, Biophysics Reports, 5 (2019), 43-59.

[22] V. Zderic,S. Vaezy, R.M. Martin, J.I. Clark, *Ocular drug delivery using 20-kHz ultrasound* , Ultrasound in Medicine and Biology, 28(2002),823–829.

[23] V. Zderic, J. I. Clark, R. Martin, S. Vaezy,*Ultrasound-enhanced trascorneal drug delivery*, Cornea, 23 (2004), 804-811.

[24] V. Zderic, J. I. Clark, S. Vaezy,*Drug delivery into the eye with the use of ultrasound*, Journal of Ultrasound in Medicine, 23 (2004), 1349-1359.

E. Azhdari
Department of Mathematics, Salman Farsi University of Kazerun, Kazerun, Iran
E-mail address: e.azhdari@kazerunsfu.ac.ir

E. Emami
Department of Mathematics, Faculty of Sciences, Fasa University, Fasa, Iran
E-mail address: emami@fasau.ac.ir

J. A. Ferreira
University of Coimbra, CMUC, Department of Mathematics, Coimbra, Portugal
E-mail address: ferreira@mat.uc.pt